VERSITA

CELLULAR & MOLECULAR BIOLOGY LETTERS
Volume 12 (2007) pp 176 - 191
http://www.cmbl.org.pl

DOI: 10.2478/s11658-007-0003-4

Received: 26 May 2006
Revised form accepted: 26 September 2006
Published online: 19 January 2007

MICROARRAY ANALYSIS REVEALS THE ROLE OF MATRIX METALLOPROTEINASES IN MOUSE EXPERIMENTAL AUTOIMMUNE MYOCARDITIS INDUCED BY CARDIAC MYOSIN PEPTIDES

QIZHU TANG[1]*, JI HUANG[1], HAIYAN QIAN[2], RAN XIONG[1], DIFEI SHEN[1], HUI WU[1], ZHOUYAN BIAN[1] and XIAOHONG WEI[1]
[1]Department of Cardiology, Renmin Hospital of Wuhan University, 430060 Wuhan, P.R. China, [2]Department of Cardiology, Fuwai Hospital and Cardiovascular Institute, Chinese Academy of Medical Science and Peking Union Medical College, 100037 Beijing, P.R. China

Abstract: Autoimmune myocarditis develops after the presentation of heart-specific antigens to autoaggressive $CD4^+$ T cells and after inflammation has infiltrated the tissues. To shed light on global changes in the gene expression of autoimmune myocarditis and to gain further insight into the molecular mechanisms underlying the genesis of myocarditis, we conducted a comprehensive microarray analysis of mRNA using an experimental mouse autoimmune myocarditis model via immunization with α-myosin heavy chain-derived peptides. Of over 39,000 transcripts on a high density oligonucleotide microarray, 466 were under-expressed and 241 over-expressed by ≥ 1.5-fold compared with the controls in BALB/C mouse with autoimmune myocarditis. In this paper, we list the top 50 up-regulated genes related to the immune response. These altered genes encode for leukocyte-specific markers and receptors, the histocompatibility complex, cytokines/receptors, chemokines/receptors, adhesion molecules, components of the complement cascade, and signal transduction-related molecules. Interestingly, matrix metalloproteinases (MMPs)

* Author for correspondence; e-mail address: qzhtang@yahoo.com, fax: (86)-27-88083385

Abbreviations used: CFA – complete Freund's adjuvant; EAM – experimental autoimmune myocarditis; ECM – extracellular matrix; MCP – monocyte chemoattractant protein; MHC – major histocompatibility complex; MIP – macrophage inflammatory protein; MMP – matrix metalloproteinase; PBS – phosphate buffered solution; RT-PCR – reverse transcriptase-polymerase chain reaction; TIMPs – tissue inhibitors of metalloproteinases

such as MMP-3 and MMP-9 were up-regulated, as further revealed by the reverse transcriptase-polymerase chain reaction (RT-PCR) and immuno-histochemistry assays. This indicates that MMPs may act as major regulators of the cytokine profile. Together, these findings provide new insight into the molecular events associated with the mechanism of the autoimmune genesis of myocarditis.

Key Words: Autoimmune, Matrix metalloproteinases, Microarray, Myocarditis

INTRODUCTION

Myocarditis is a frequent cause of cardiac failure in young adults. Autoimmunity plays an important role in this condition and contributes to the progression to cardiomyopathy [1]. Animal models are employed to study the pathogenesis of myocarditis using modes including infection-triggered inflammation and autoimmune-associated inflammation [2, 3]. Autoimmune myocarditis is dependent on $CD4^+$ T cells recognizing heart-specific peptides together with major histocompatibility complex (MHC) class II molecules on antigen-presenting cells. Experimental autoimmune myocarditis (EAM) can be induced in susceptible mouse strains by immunization with purified cardiac myosin [4] or α-myosin heavy chain-derived peptides [5, 6] together with complete Freund's adjuvant (CFA). This model of EAM is similar to human myocarditis in histology, including the recruitment of lymphocytes, macrophages, and neutrophils accompanying myocardial necrosis [2, 7-10]. However, the molecular mechanisms of the genesis of autoimmune myocarditis are still not clear.

The analysis of gene expression with microarrays allows for the simultaneous examination of the expression levels of thousands of genes. Novel genes, not previously described in a specific experimental model, may be identified by this methodology. Microarray studies of some experimental autoimmune diseases such as autoimmune encephalomyelitis have recently been reported on, and over 100 immune-related transcripts were consistently differentially expressed [11, 12]. Microarray analysis has also been used in cardiac hypertrophy [13] and myocardial infarction models [14] to characterize broad patterns of gene expression. In this study, we used microarray analysis to explore the changes in gene expression that occur between EAM and normal control mice allowing the identification and functional characterization of the immune-related genes involved in the pathogenesis of myocarditis.

MATERIALS AND METHODS

Immunization and tissue harvesting

A murine heart muscle-specific peptide derived from α-myosin-heavy chain-derived peptide (myhc-614-629 [Ac-SLKLMATLFSTYASAD-OH]) was used as the antigen [15]. The peptide (purity, > 95%; AC Scientic, Inc. China) was dissolved in phosphate buffered solution (PBS) (1 mg/ml) and emulsified in an

equal volume of Freund's complete adjuvant (1 mg/ml, Sigma-Aldrich Chemicals, St. Louis, MO). Nine male BALB/c mice at the age of 6-8 weeks were immunized subcutaneously with 100 µg/0.2 ml on day 0 and day 7. Nine gender and age-matched mice were used as sham-immunized controls, injected with CFA emulsified with PBS alone. On day 0, before immunization, all the mice were injected intraperitoneally with 400 ng pertussis toxin diluted in 400 µl distilled water, 0.015 M Tris, 0.5 M NaCl, and 0.017% (v/v) Triton X-100 (pH 7.5). Twenty one days after the immunization, the mice were killed and their hearts were removed to be dissected and rinsed free of blood, and either snap-frozen in liquid nitrogen or fixed with 10% (v/v) formalin for pathological analysis. Frozen samples then underwent RNA isolation for microarray analysis and RT-PCR. All the experiments were performed according to the institutional guidelines for animal care and treatment which is in line with guidelines for the care and use of animals (NIH 1996 No. 85-23).

Histopathology

As mentioned above, 21 days after the immunization, the hearts were removed, fixed in formalin for 24 hours, embedded in paraffin, and stained with hematoxylin and eosin. Myocarditis was determined by identifying both infiltrating mononuclear cells and myocyte necrosis. The score of myocardial inflammation was on a semiquantitative scale using grades from 0 to 4 as previously described [4]. 0 indicated no inflammatory infiltrates, 1 was small foci of inflammatory cells between myocytes, 2 was larger foci of over 100 inflammatory cells, 3 was > 10% of a cross-section involved and 4 was > 30% of a cross section involved.

RNA preparation and Affymetrix microarray hybridization

All the experiments were performed using Affymetrix Mouse Genome 430A 2.0 Array oligonucleotide arrays, as described at http://www.affymetrix.com/ products/arrays/specific/mouse430a_2.affx. Total RNA was extracted from the frozen bi-ventricular tissues using TRIzol reagent and RNeasy spin columns following homogenization. RNA quality and integrity were determined by spectrophotometer and gel electrophoresis. The total RNA from each sample was used to prepare biotinylated target RNA, with minor modifications from the manufacturer's recommendations, given at http://www.affymetrix.com/ support/ technical/manual/expression_manual.affx. Briefly, 10 µg of mRNA was used to generate first-strand cDNA by using a T7-linked oligo (dT) primer. After second-strand synthesis, *in vitro* transcription was performed with biotinylated UTP and CTP (Enzo Diagnostics), resulting in an approximately 100-fold amplification of RNA. A complete description of the procedures is available at http://bioinf.picr.man.ac.uk/mbcf/downloads/GeneChip_Target_Prep_Protocol_ CRUK_v_2.pdf. The target cDNA generated from each sample was processed as per the manufacturer's recommendations, using an Affymetrix GeneChip Instrument System, as described at http://www.affymetrix.com/support/ technical/manual/expression_manual.affx. Briefly, spike controls were added to

10 µg fragmented cDNA before overnight hybridisation. Arrays were then washed and stained with streptavidin-phycoerythrin, before being scanned with an Affymetrix GeneChip scanner. A complete description of these procedures is available at http://bioinf.picr.man.ac.uk/mbcf/downloads/GeneChip_Hyb_Wash_Scan_Protocol_v_2_web.pdf. Each sample was screened and found to be free from mycoplasma contamination. Additionally, the quality and amount of starting RNA was confirmed using an agarose gel. After scanning, array images were assessed by eye to confirm the scanner alignment and the absence of significant bubbles or scratches on the chip surface. The 3'/5' ratios for GAPDH and beta-actin were confirmed to be within the acceptable limits, and BioB spike controls were found to be present on all the chips, with BioC, BioD and CreX also present in increasing intensity. The quality control design reduced the process variability thanks to its redundancy, ensuring consistency for the correlation coefficient, change of detection call, and rate of false change call. The change of detection call from present (P) to absent (A), and conversely, A to P was < 10%, and the false change of comparisons between two samples in the same group was < 2%. RNA isolated from individual mice was hybridized on individual chips, and each experimental grouping consisted of three chips.

Affymetrix data analysis

When scaled to a target intensity of 500 (using Affymetrix MAS 5.0 array analysis software), the scaling factors for all the arrays were within the acceptable limits, as were the background, Q values, and mean intensities. The MAS 5.0 detection algorithm calculates the detection P-value using 16 pairs of perfect match (PM) and mismatch (MM) probes, assigning each a P or A call. Our P-values fell within < 0.04 for a P call and > 0.06 for an A call; values between 0.04 and 0.06 were considered marginal. The signal, a quantitative metric value calculated for each probe set, represents the relative expression of a transcript. The fold change and P-value measure the signal variation of a single gene between the baseline and experimental arrays. MAS 5.0 uses Wilcoxon's Signed Rank test to calculate this variation, assigning an increase ($P < 0.0025$), decrease ($P > 0.9975$), or no change call (P between 0.0025 and 0.9975) to each gene. The preprocessed data is stored as log2-transformed real signal numbers. Genes were considered up- or down-regulated if the magnitude of change was 1.5-fold or greater.

Semiquantitative PCR amplifications

Reverse-transcriptase polymerase chain reaction (RT-PCR) was used to detect the transcript levels of MMP-3, MMP-9, TIMP-1, IL-1β, and TNF-α on day 21 after immunization. The total RNA was isolated and purified by RNA-TRIZOL extraction as described above. We used the same samples as in the above microarray analysis. The forward and reverse sequence primers for MMP-3, MMP-9, TIMP-1, IL-1β, and TNF-α were based on GenBank mouse sequences. A primer was also made for mouse GAPDH, which was used as an internal

control. The PCR primers and the conditions that were used to obtain the sequences are summarized in Tab. 1. 36 cycles of a 30 s denaturing step at 94ºC, a 30 s annealing step at 62ºC and a 45 s primer extension at 72ºC were followed by a final 7-min incubation at 72ºC to ensure that the PCR products were of full length. The PCR products were visualized under UV light with ethidium bromide staining in 1.5% agarose gel, and fluorescence images were captured and band density determined with software. The specific bands of PCR products were measured as optical densities (OD) using a software program. The ratio of the target amplicon (OD) to the GAPDH amplicon (OD) was calculated as the relative mRNA level. Three samples were measured in each experimental group in duplicate in a minimum of two independent experiments.

Tab. 1 Primer sequences used for semi-quantitative RT-PCR.

mRNA	5' Region	3' Region	Annealing T (ºC)	Product size (bp)
MMP-3	ggcttcagtaccttcccagg	gcagcaaccaggaataggtt	59.0	356
MMP-9	tgggcaaaggcgtcgtga	cacagctctcctgccgagtt	59.2	406
TIMP-1	cgaatcaacgagaccaccttat	ccgtccacaaacagtgagtgtca	60.8	370
IL-1β	gtaatgaaagacggcacac	cctaatgtccccttgaatca	60.0	510
TNF-α	agaaaggggattatgg	gaggttcagtgatgtaggcga	58.8	591
GAPDH	gaaacctgccaagtatgatg	accaggaaatgagcttgagc	55.0	191

Immunohistochemistry

Samples were fixed in 4% formaldehyde and embedded in paraffin wax. 4 μm sections were cut before deparaffinization and rehydration. Slides with these tissue sections were incubated in 3% hydrogen peroxide to block endogenous peroxidase activity, and then in 5% normal goat serum to block non-specific binding. The sections were incubated for 1 h at room temperature with either rabbit anti-mouse MMP-3 antibody (Boster, China), goat anti-mouseMMP-9 or TIMP-1 antibody (Santacruz, America). The control slides were incubated with normal Bovine Calf Sera. Anti-rabbit biotinylated secondary antibody (Beijing Zhongshan Golden Bridge Biotechnology Co., LTD. China) was applied to the sections for 15 min at 37ºC, followed by the avidin/biotinylated peroxidase complex for another 15 min at 37ºC. The sections were incubated with chromogenic substrate diaminobenzidine (DAB) for 5 min, and then counterstained in haematoxylin and mounted in an aqueous mounting medium. Each slide was screened under high-power light microscopy, and 6 independent fields of vision were selected randomly. We used HPIAS-2000 image analysis software to analyze the optical density of every field of vision.

Statistical analyses

For quantitative analysis, all the data was expressed as means ± SD. The significance of differences in the data was evaluated using the two-sided Student's *t*-test. A value of $P < 0.05$ was considered statistically significant.

RESULTS

Peptide-immunized autoimmune myocarditis

Myocarditis was confirmed histologically by the prominent cellular infiltrates in the ventricular sections from mice hearts 21 days after peptide immunization (Fig. 1A). The control tissues were infiltrated by few monocytes (Fig. 1B). This recapitulates histological patterns seen previously in myosin-induced autoimmune myocarditis in mice [8]. The heart weight and heart weight to body weight ratios were significantly changed in peptide-immunized mice relative to the controls (Tab. 2).

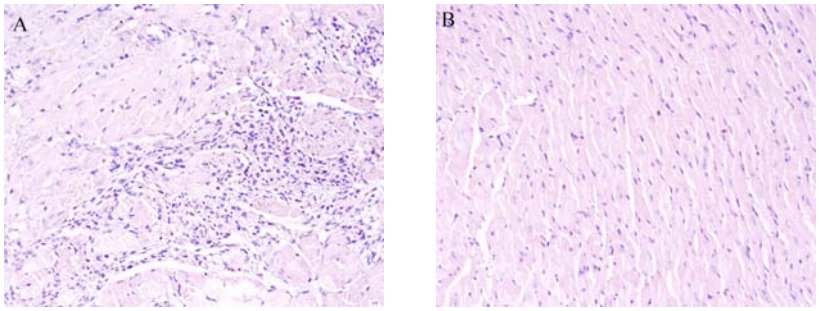

Fig. 1. Histological examinations of acute peptide-immunized myocarditic mouse heart tissues. (A) Representative histopathology in a mouse with myocarditis. (B) Histopathology in the control. Cardiac inflammation was defined as a mononuclear cell infiltrate with myocytes necrosis. (Original magnification 200×).

Tab. 2. Heart weight and histopathology score in mice.

Group	Heart weigh [g]	Body weight [g]	Heart weight/ body weight	Microscopic score
PBS/CFA	0.089 ± 0.012	23.0 ± 1.98	$3.97\times10^{-3} \pm 2.22\times10^{-4}$	0.7 ± 0.2
Peptide/CFA	0.112 ± 0.025$^{\#}$	22.8 ± 2.11	$4.93\times10^{-3} \pm 1.75\times10^{-4}$ $^{\#}$	3.5 ± 0.6*

$^{\#}P < 0.05$ vs. PBS/CFA; $^{*}P < 0.01$ vs. PBS/CFA

Identification of genes that are differentially expressed by the EAM and control mice

In the EAM mice as compared with the controls 241 transcripts were significantly up-regulated and 466 transcripts were down-regulated. Of these differentially expressed genes, 518 have annotations based on process hierarchy. The distribution of these genes is: 32.38% cellular component, 34.85% molecular function and 32.77% biological process. Gene ontology analysis identified genes within the following functional groups: regulation of transcription, DNA-dependent (59), transport (49), protein amino acid phosphorylation (28), development (27), intracellular signaling cascade (24), biological, process

Tab. 3. Top 50 up-regulated immune-related genes.

Gene title	Gene symbol	GO biological process description	Fold change
MHCs and related molecules			
histocompatibility 2, class II antigen A, alpha	h2-Aa	antigen presentation	32.0
histocompatibility 2, class II antigen A, beta 1	h2-Ab1	antigen presentation	28.6
histocompatibility 2, class II antigen E alpha	h2-Ea	antigen presentation	64.0
histocompatibility 2, class II antigen E beta	h2-Eb1	antigen presentation	22.4
histocompatibility 2, class II, locus Mb1 / histocompatibility 2, class II, locus Mb2	h2-dmb1/b2	antigen presentation	32.0
histocompatibility 2, T region locus 24	h2-t24	antigen presentation	52.0
Chemokines and receptors			
chemokine (C-C motif) ligand 5	ccl5	immune response	8.6
chemokine (C-C motif) receptor 2	ccr2	inflammatory response	6.2
chemokine (C-C motif) receptor 5	ccr5	immune response	8.6
chemokine (C-X-C motif) ligand 7	cxcl7	immune response	8.8
chemokine (C-X-C motif) receptor 4	cxcr4	chemotaxis, defense response	2.4
chemokine (C-C motif) ligand 12	ccl12	immune response	8.4
chemokine (C-C motif) ligand 21	ccl21	immune response	10.2
chemokine (C-X-C motif) ligand 14	cxcl14	immune response	2.6
Cytokines and related molecules			
insulin-like growth factor binding protein 3	lgfbp3	regulation of cell growth	3.4
interferon inducible GTPase 1	ligp1	GTPase activity	2.2
interferon regulatory factor 8	irf8	regulation of transcription	2.6
interferon-induced protein with tetratricopeptide repeats 1	ifit1	immune response	8.0
interleukin 1 family, member 8	il1f8	cytokine	12.8
interleukin 12b	il12b	cytokine	3.6
tumor necrosis factor (ligand) superfamily, member 13	tnfsf13	immune response	16.0
tumor necrosis factor receptor superfamily member 12a	tnfrsf12a	receptor activity	8.4
tumor necrosis factor receptor superfamily, member 1b	tnfrsf1b	apoptosis	18.6
tumor necrosis factor alpha	tnfa	inflammation response	8.6
transforming growth factor beta receptor 1	tgfbr1	phosphorylation	3.0
vascular endothelial growth factor A	vegfa	angiogenesis	12.8

Gene title	Gene symbol	GO biological process description	Fold change
Cell adhesion- and matrix metalloproteinase-related molecules			
stabilin 1	stab1	cell adhesion	5.6
thrombospondin 4	thbs 4	cell adhesion	3.4
vascular cell adhesion molecule 1	vcam1	cell adhesion	10.6
matrix metallopeptidase 9	mmp9	proteolysis	7.4
matrix metallopeptidase 3	mmp3	proteolysis	6.0
Complement cascade-related molecules			
complement 3	c3	inflammatory response	4.0
decay-accelerating factor 1	daf1	complement activation, classical pathway	7.6
Other immune-related molecules			
CD14 antigen	cd14	inflammatory response	16.0
CD28 antigen	cd28	immune response	4.0
immunoglobulin heavy chain 6 (heavy chain of IgM)	igh-6	antigen processing	6.4
leukocyte common antigen	lca	immune response	8.4
leukocyte-specific transcript 1	lst1	immune response	5.4
macrophage activation 2 like	mpa2l	immune response	3.4
proteosome (prosome, macropain) subunit, beta type 9 (largemultifunctio-nal peptidase 2)	psmb9	antigen processing	3.4
endothelial differentiation, sphingolipid G-protein-coupled receptor, 3	edg3	inflammatory response	4.0
Signal transduction, transcription and translation factors			
B-cell translocation gene 2, antiproliferative	btg2	regulation of transcription	12.2
HS1 binding protein 3	hs1bp3	cell surface receptor-linked signal transduction	6.2
Ia-associated invariant chain	ii	intracellular protein transport	2.0
interleukin-1 receptor-associated kinase 4	irak4	signal transport	9.0
nuclear factor of activated T-cells, cytoplasmic, calcineurin-dependent 2	nfatc2	regulation of transcription	16.0
nuclear factor of kappa light chain gene enhancer in B-cell inhibitor alpha	nfkbia	protein import into the nucleus	12.6
Miscellaneous genes			
gap junction membrane channel protein alpha 1	gja1	cell communication	3.8
granzyme A	gzma	proteolysis	5.0
tnf receptor-associated factor 7	traf7	apoptosis	6.0

unknown (22), signal transduction (20), cell adhesion (18), G-protein-coupledreceptor protein signaling pathway (17), proteolysis and peptidolysis (16), metabolism (15), immune response (81), cell growth and/or maintenance (13), cell cycle (11), ion transport (11), regulation of cell cycle (10), apoptosis (10), protein transport (9), heterophilic cell adhesion (9), antigen processing (9), and some genes associated with other biological processes (Fig. 2).

In the top 50 up-regulated immune-related genes (Tab. 3), there are several groups: T-cell related proteins (CD28 antigen), MHCs and related molecules (histocompatibility 2, class II antigen A, alpha), cytokines/chemokines and receptors (CCR2, CXCR4, CCR5, CXCL7, CXCL14), adhesion molecules (VCAM-1, stabilin 1, Thrombospondin 4), and matrix metalloproteinases (MMP-3, MMP-9).

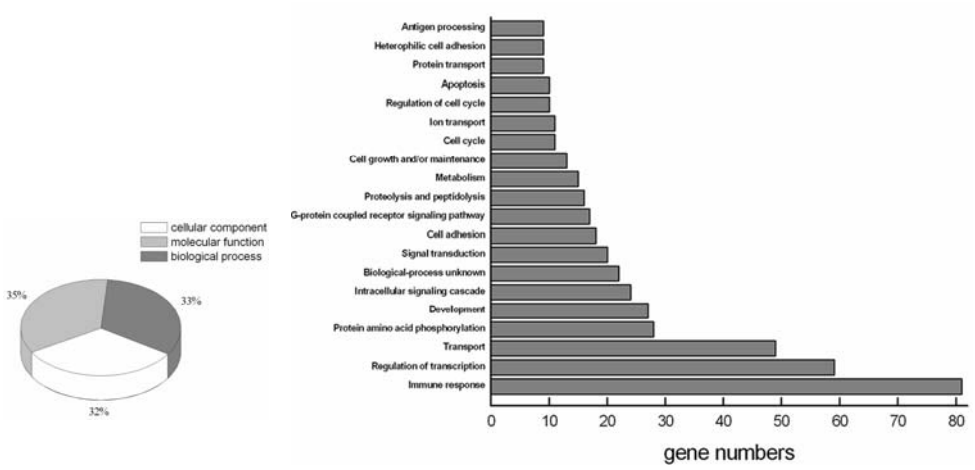

Fig. 2. Identification of the genes that are differentially expressed by the EAM and control mice based on Gene Ontology Analysis.

The validation of microarray analysis using PT-PCR

To confirm (and extend) the affymetrix microarray dataset, IL-1β, TNF-α, MMP-3 and MMP-9 were selected for RT-PCR analysis. RT-PCR analysis demonstrated a significant increase in the expressions of inflammatory cytokines such as IL-1β ($P < 0.01$) and TNF-α ($P < 0.01$) in EAM mice relative to the control (Fig. 3A). In addition, the expression of matrix metalloproteinases such as MMP-3 ($P < 0.01$) and MMP-9 ($P < 0.01$) was also significant elevated in EAM mice relative to the control (Fig. 3B). These results demonstrate that microarray analysis data correlates well with the PT-PCR data. The results of recent studies indicated that myocardial collagen can be caused by imbalances between myocardial MMPs and TIMPs [16, 17]. Therefore, we also examined one of the tissue inhibitors of metalloproteinases (TIMPs), TIMP-1, which potently inhibits the activity of most MMPs, with the exception of MMP-2 and

membrane-type MMP (MT1-MMP) [18]. The expression of TIMP-1 ($P < 0.01$) significantly decreased in EAM mice compared with the controls (Fig. 3C). Fig. 3D shows the graphical representation of the densitometric analyses.

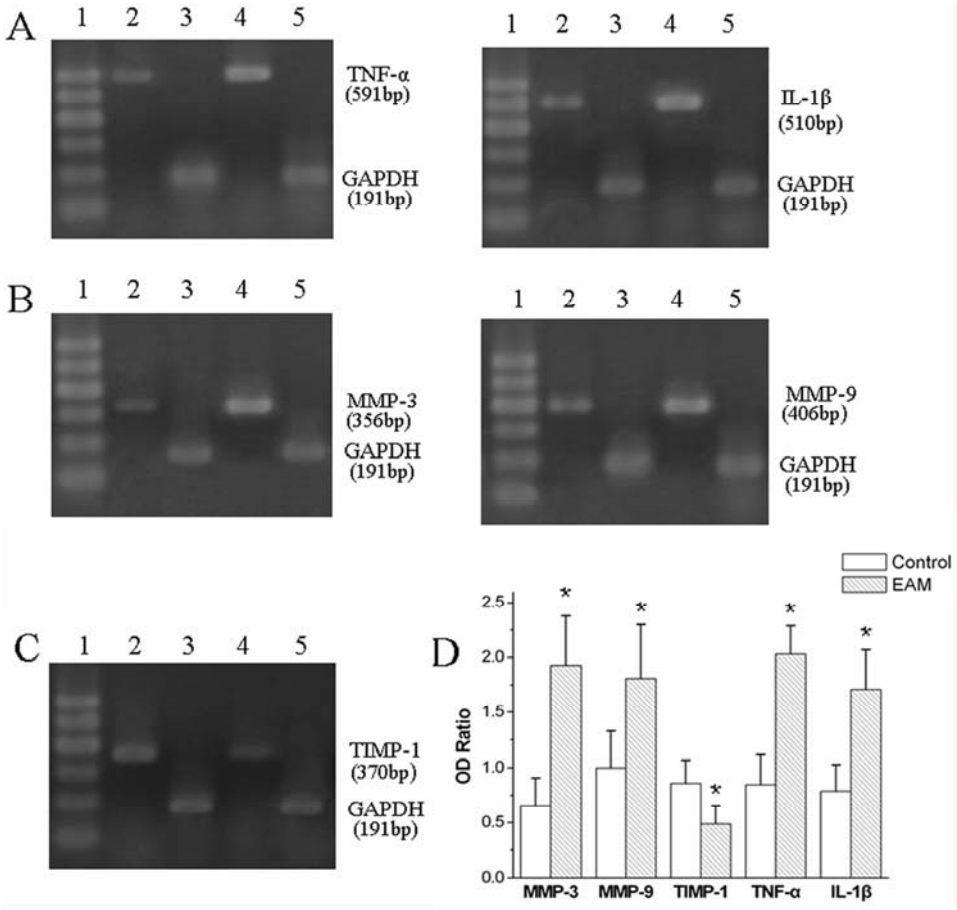

Fig. 3. Transcriptional levels of IL-1β, TNF-α, MMP-3, MMP-9 and TIMP-1. RT-PCR for (A) IL-1β and TNF-α, and (B) MMP-3 and MMP-9 in sham- and peptide-immunized mouse hearts. The expression was up-regulated on day 21. (C) RT-PCR for TIMP-1 in sham- and peptide-immunized mouse hearts. The expression was down-regulated on day 21. (D) Densitometric analyses of the bands (mean ± SD) showed a significant change in IL-1β, TNF-α, MMP-3, MMP-9 and TIMP-1 expression relative to the controls, *$P < 0.01$ vs. the control. Lane 1 is the marker, lanes 2 and 3 show the control group, and lanes 4 and 5 show the EAM group.

Immunohistochemistry revealed changes in the expression of matrix metalloproteinases in the EAM mice

The changes in the myocardial gene expression profile were consistent with the pathological findings on inflammatory cell infiltration within the hearts of the

EAM mice. However, the Affymetrix microarray analyses also suggested a previously unappreciated change in the extracellular matrix (ECM) component to this model. Therefore, a more extensive immunohistochemical characterization of ECM in myocarditis was performed. We carried out immunostaining for MMP-3, MMP-9 and TIMP-1 to validate the mRNA expression in the heats of the EAM mice. Fig. 4A, D and H respectively show MMP-3, MMP-9 and TIMP-1 positivity within the cardiomyocytes and vasculature in sham hearts. On day 21 after immunization, the tissue sections immunostained for MMP-3 (Fig. 4B) and MMP-9 (Fig. 4E) both showed increased expression in the hearts of EAM mice relative to the controls,

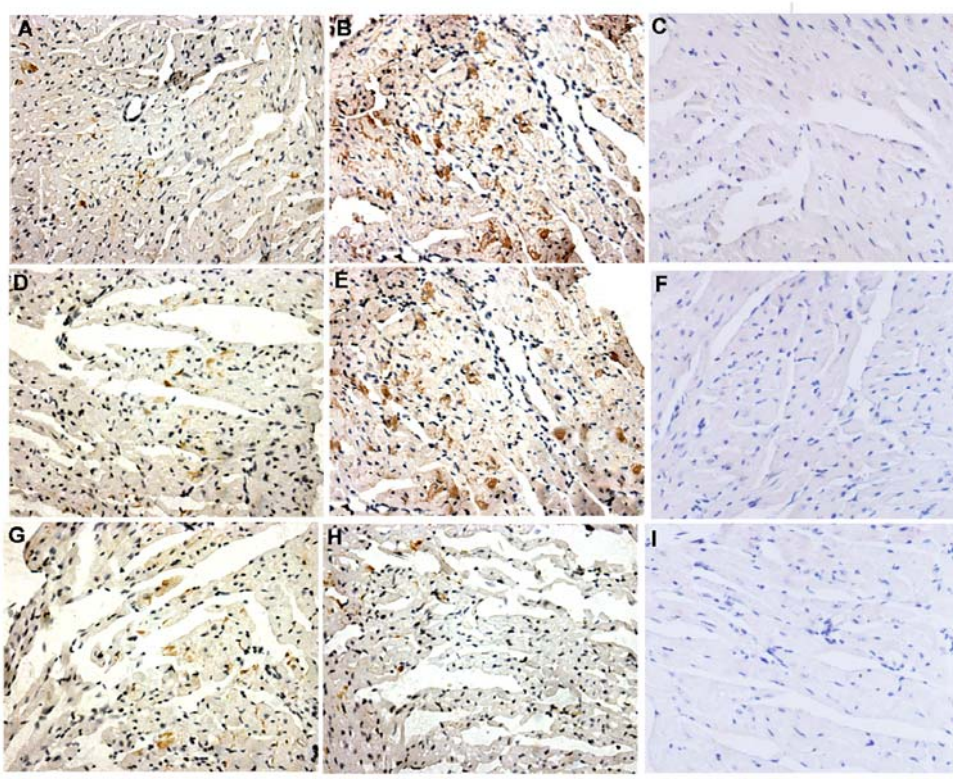

Fig. 4. Immunohistochemistry for MMP-3 (A and B), MMP-9 (C and D), and TIMP-1 (E and F) in the control and EAM groups on day 21. Panels A, D and G represent the positive control. Panels C, F and J represent the negative control. Panels B, E and H represent the EAM group. The expression of MMP-3 and MMP-9 is up-regulated, while the expression of TIMP-1 is down-regulated. (Original magnification × 400).

particularly in and around the necrotic foci, but also in the resident cardiac cells of normal regions, while TIMP-1 (Fig. 4I) was expressed less in the hearts of the EAM mice than in the controls. The semi-quantified levels of expression of

MMP-3, MMP-9 and TIMP-1 using the integrated optical density values are listed in Tab. 4. These results were concordant with their mRNA expression. The mRNA expression of these genes as demonstrated by microarray and RT-PCR analysis was in agreement with the protein expression data.

Tab. 4. Semi-quantified levels of expression of MMP-3, MMP-9 and TIMP-1 using the integrated optical density values.

	OD values		
	MMP-3	MMP-9	TIMP-1
Immune group	1.99 ± 0.38**	1.19 ± 0.42*	0.50 ± 0.19*
Control group	0.89 ± 0.27	0.73 ± 0.36	0.86 ± 0.24

*vs. control group $P < 0.05$; **vs. control group $P < 0.01$.

DISCUSSION

Although there is a model of autoimmune myocarditis in mice immunized by a myocardium-specific peptide derived from the α-myosin-heavy chain [3], the precise molecular mechanisms leading to myocarditis are not clear. By using the murine Affymetrix high-density oligonucleotide microarray, we were able to describe here for the first time the overall differential transcriptional changes in the expressions of genes in the hearts of the EAM mice compared with the controls. These analyses allowed us to identify genes that are crucial in the induction of acute EAM. These include leukocyte-specific antigens, T-cell receptors, cytokines and their receptors, chemokines and their receptors, and adhesion molecules (Tab. 3). Histopathologic staining and levels of accumulated transcripts for genes associated with inflammation confirm the infiltration in the hearts of the EAM mice. The pathogenesis of EAM is closely linked to $CD4^+$ T cells and macrophages [19, 20]. The induction of autoimmune myocarditis increased the expression of myosin MHC class II in the heart and enhanced their antigen-presenting cell functions [5]. Our findings demonstrated that the expression of MHC class II molecules was up-regulated in microarray analysis. We also found components of the complement cascade, such as C3, were up-regulated. The C3 component was found to be critical for the development of EAM. Depletion of C3 through its activation by the administration of cobra venom factor resulted in impaired IgG responses and prevented myocarditis in mice immunized with cardiac myosin [21]. It has been reported that various inflammatory cytokines and proinflammatory chemokines are involved in the pathogenesis of EAM, including TNF-α, IL-12, macrophage inflammatory protein-1 α (MIP-1 α), MIP-2, monocyte chemoattractant protein-1 (MCP-1), MCP-3 and cytokine-regulated gene-2 [22, 23]. Blocking MCP-1 or MIP-1α with monoclonal antibodies significantly reduced the severity of myocarditis in BALB/c mice immunized with cardiac myosin. Similar results were obtained with CCR2–/– and CCR5–/– mice; furthermore, in CCR2–/– mice, not only the

severity but also the prevalence of the disease was reduced [24]. Our results demonstrated that in the top 50 up-regulated immune-related genes, the levels of IL-12, IL-1β, TNF-α, CCL5, CCR5, CCR2, CCL21 and other chemokines increased.

This study also revealed an increased expression of matrix metalloproteinases including MMP-3 and MMP-9. Tissue inhibitors of metalloproteinases such as TIMP-1 were down-regulated. The myocardial inflammatory reaction was accompanied by a significant up-regulation of MMP-3 and MMP-9, but a down-regulation of TIMP-1 at the mRNA and protein levels. MMP-2, MMP-3 and MMP-9 have been implicated in cardiac remodeling in human dilated cardiomyopathy [25, 26]. It has been reported that most immune cells secreted MMP-9 in order to aid matrix degradation during migration [27], and these cells also secreted proinflammatory cytokines such as TNF-α and interleukin-1, which may trigger further MMP up-regulation [28]. MMP-9 has been suggested to play a role in cytokine processing via the cleavage and release of active molecules such as TGF-β and interleukins [29]. These activated MMPs can be inhibited by interaction with naturally occurring, specific inhibitors, the TIMPs, which are expressed by a variety of cell types and are present in most tissues and body fluids, resulting in the influx of immune cells and matrix remodeling. TIMP-1 has been implicated in various heart diseases, such as MI and heart failure [30, 31]. In a model of myocarditis induced by coxsackievirus B3 (CVB3), MMP-2, MMP-9 and MMP-12 transcription was increased and TIMP-3 and TIMP-4 expression was down-regulated [32]. In another model of myocarditis induced by CVB3, Li *et al.* [33] demonstrated that the levels of mRNAs and protein for MMP-3 and MMP-9 were up-regulated, whereas TIMP-1 and TIMP-4 were down-regulated, and this was associated with significantly increased mRNA levels of interleukin 1β, tumor necrosis factor-α, transforming growth factor-β1 and interleukin-4. The regulation of MMP-3 and MMP-9 in myocarditic hearts is due to inhibition by TIMP-1. In this study, the fact that the levels of MMP3 and MMP9 increased during the acute inflammatory phase concurrently with the TNF-α and IL-1β increment suggests that they modulate inflammation and ECM remodeling, possibly through cytokine regulation.

In conclusion, a global feature of gene expression occurring in autoimmune myocarditis mice immunized by specific α-myosin-heavy chain-derived peptide was demonstrated by microarray analysis. These findings were confirmed by RT-PCR and immunohistochemical analysis, and suggest that MMPs not only function in the degradation of the matrix, but also act as major regulators of the cytokine profile, contributing to myocardial injury and remodeling during the progression of myocarditis.

REFERENCES

1. Caforio, A.L., Mahon, N.J. and McKenna, W.J. Cardiac autoantibodies to myosin and other heart-specific autoantigens in myocarditis and dilated cardiomyopathy. **Autoimmunity** 34 (2001) 199-204.
2. Neumann, D.A., Rose, N.R., Ansari, A.A. and Herskowitz, A. Induction of multiple heart autoantibodies in mice with coxsackievirus B3- and cardiac myosin-induced autoimmune myocarditis. **J. Immunol.** 152 (1994) 343-350.
3. Kodama, M., Matsumoto, Y., Fujiwara, M., Masani, F. and Shibata, A. A novel experimental model of giant cell myocarditis induced in rats by immunization with cardiac myosin fraction. **Clin. Immunol. Immunopathol.** 57 (1990) 250-262.
4. Neu N., Rose, N.R., Beisel, K.W., Herskowitz, A., Gurri, G.G. and Craig, S.W. Cardiac myosin induces myocarditis in genetically predisposed mice. **J. Immunol.** 139 (1987) 3630-3636.
5. Pummerer, C.L., Luze, K., Grässl, G., Bachmaier, K., Offner, F., Burrell, S.K., Lenz, D.M., Zamborelli, T.J., Penninger J.M. and Neu, N. Identification of Cardiac Myosin Peptides Capable of Inducing Autoimmune Myocarditis in BALB/c Mice. **J. Clin. Invest.** 97 (1996) 2057-2062.
6. Eriksson, U., Ricci, R., Hunziker, L., Kurrer, M.O., Oudit, G.Y., Watts, T.H., Sonderegger, I., Bachmaier, K., Kopf, M. and Penninger, J.M. Dendritic cell-induced autoimmune heart failure requires cooperation between adaptive and innate immunity. **Nat. Med.** 9 (2003) 1484-1490.
7. Pummerer, C., Berger, P., Fruhwirth, M., Ofner, C. and Neu, N. Cellular infiltrate, major histocompatibility antigen expression and immunopathogenic mechanisms in cardiac myosin-induced myocarditis. **Lab. Invest.** 65 (1991) 538-547.
8. Smith, S.C. and Allen, P.M. Myosin-induced acute myocarditis is a T cell-mediated disease. **J. Immunol.** 147 (1991) 2141-2147.
9. Izumi, T., Suzuki, K., Saeki, M., Ookura, Y., Hirono, S., Inomata, T., Hanawa, H. and Kodama, M. An ultrastructural study on experimental autoimmune myocarditis with special reference to effector cells. **Eur. Heart J.** 16(suppl O) (1995) 75-77.
10. Wang, Y., Afanasyeva, M., Hill, S.L. and Rose, N.R. Characterization of murine autoimmune myocarditis induced by self and foreign cardiac myosin. **Autoimmunity** 31 (1999) 151-162.
11. Lock, C., Hermans, G., Pedotti, R., Brendolan, A., Schadt, E., Garren, H., Langer-Gould, A., Strober, S., Cannella, B., Allard, J., Klonowski, P., Austin, A., Lad N., Kaminski, N., Galli, S.J., Oksenberg, J.R., Raine, C.S., Heller, R. and Steinman, L. Gene-microarray analysis of multiple sclerosis lesions yields new targets validated in autoimmune encephalomyelitis. **Nat. Med.** 8 (2002) 500-508.
12. Matejuk, A., Dwyer, J., Zamora, A., Vandenbark, A.A. and Offner, H. Evaluation of the effects of 17beta-estradiol (17beta-e2) on gene expression

in experimental autoimmune encephalomyelitis using DNA microarray. **Endocrinology** 143 (2002) 313-319.
13. Aronow, B.J., Toyokawa, T., Canning, A., Haghighi, K., Delling, U., Kranias, E., Molkentin, J.D. and Dorn, G.W. Divergent transcriptional responses to independent genetic causes of cardiac hypertrophy. **Physiol. Genomic.** 6 (2001) 19-28.
14. Stanton L.W., Garrard L.J., Damm D., Garrick B.L., Lam A., Kapoun A.M., Zheng, Q., Protter, A.A., Schreiner, G.F. and White T. Altered patterns of gene expression in response to myocardial infarction. **Circ. Res.** 86 (2000) 939-945.
15. Cihakova, D., Sharma, R.B., Fairweather, D., Afanasyeva, M. and Rose, N.R. Animal Models for Autoimmune Myocarditis and Autoimmune Thyroiditis. in **Autoimmunity: methods and protocols** (Perl, A., Ed.), New Jersey, Humana Press, 2004 pp 175-193.
16. Ducharme, A., Frantz, S., Aikawa, M., Rabkin, E., Lindsey, M., Rohde, L.E., Schoen, F.J., Kelly, R.A., Werb, Z., Libby, P. and Lee, R.T. Targeted deletion of matrix metalloproteinase-9 attenuates left ventricular enlargement and collagen accumulation after experimental myocardial infarction. **J. Clin. Invest.** 106 (2000) 55-62.
17. Kim, H.E., Dalal, S.S., Young, E. Legato, M.J., Weisfeldt, M.L. and D'Armiento, J. Disruption of the myocardial extracellular matrix leads to cardiac dysfunction. **J. Clin. Invest.** 106 (2000) 857-866.
18. Creemers, E.E.J.M., Cleutjens, J.P.M., Smits, J.F.M. and Daemen, M.J.A.P. Matrix metalloproteinase inhibition after myocardial infarction: A new approach to prevent heart failure? **Circ. Res.** 89 (2001) 201-210.
19. Kodama, M., Zhang, S., Hanawa, H. and Shibata, A. Immunohistochemical characterization of infiltrating mononuclear cells in the rat heart with experimental autoimmune giant cell myocarditis. **Clin. Exp. Immunol.** 90 (1992) 330-335.
20. Hanawa, H., Tsuchida, M., Matsumoto, Y., Watanabe, H., Abo, T., Sekikawa, H., Kodama, M., Zhang, S., Lzumi, T. and Shibata, A. Characterization of T cells infiltrating the heart in rats with experimental autoimmune myocarditis. Their similarity to extrathymic T cells in mice and the site of proliferation. **J. Immunol.** 150 (1993) 5682-5695.
21. Kaya, Z., Afanasyeva, M., Wang, Y., Dohmen, K.M., Schlichting, J., Tretter, T., Delisa, F., Holers V.M. and Rose, N.R. Contribution of the innate immune system to autoimmune myocarditis: a role for complement. **Nat. Immunol.** 2 (2001) 739-745.
22. Fuse, K., Kodama, M., Hanawa, H., Okura, Y., Ito, M., Shiono, T., Kato, K., Watanabe, K. and Aizawa, Y. Enhanced expression and production of monocyte chemoattractant protein-1 in myocarditis. **Clin. Exp. Immunol.** 124 (2001) 346-352.
23. Kurrer, M.O., Kopf, M., Penninger, J.M. and Eriksson, U. Cytokines that regulate autoimmune myocarditis. **Swiss. Med. Wkly.** 132 (2002) 408-413.

24. Göser, S., Öttl, R., Brodner, A., Dengler, T.J., Torzewski, J., Egashira, K., Rose, N.R., Katus, H.A. and Kaya, Z. Critical role for monocyte chemoattractant protein-1 and macrophage inflammatory protein-1α in induction of experimental autoimmune myocarditis and effective anti-monocyte chemoattractant protein-1 gene therapy. **Circulation** 112 (2005) 3400-3407.
25. Rouet-Benzineb, P., Buhler, J.M., Dreyfus, P., Delcourt, A., Dorent, R., Perennec, J., Crozatier, B., and Harf, A. and Lafuma, C. Altered balance between matrix gelatinases (MMP-2 and MMP-9) and their tissue inhibitors in human dilated cardiomyopathy: potential role of MMP-9 in myosin heavy chain degradation. **Eur. J. Heart. Fail.** 1 (1999) 337-352.
26. Thomas, C.V., Coker, M.L., Zellner, J.L., Handy, J.R., Crumbley, A.J. 3rd and Spinale, F.G. Increased matrix metalloproteinase activity and selective upregulation in LV myocardium from patients with end-stage dilated cardiomyopathy. **Circulation** 97 (1998) 1708-1715.
27. Van Den Steen, P.E., Wuyts, A., Husson, S.J., Proost, P., Van, D.J. and Opdenakker, G. Gelatinase B/MMP-9 and neutrophil collagenase/MMP-8 process the chemokines human GCP-2/CXCL6, ENA-78/CXCL5 and mouse GCP-2/LIX and modulate their physiological activities. **Eur. J. Biochem.** 270 (2003) 3739-3749.
28. Vreugdenhil, G.R., Wijnands, P.G., Netea, M.G., van der Meer, J.W., Melchers, W.J. and Galama, J.M. Enterovirus-induced production of proinflammatory and T-helper cytokines by human leukocytes. **Cytokine** 12 (2000) 1793-1796.
29. Sternlicht, M.D. and Werb, Z. How matrix metalloproteinases regulate cell behavior. **Annu. Rev. Cell. Dev. Biol.** 17 (2001) 463-516.
30. Gaertner, R., Jacob, M.P., Prunier, F., Angles-Cano, E., Mercadier, J.J. and Michel, J.B. The plasminogen-MMP system is more activated in the scar than in viable myocardium 3 months post-MI in the rat. **J. Mol. Cell. Cardiol.** 38 (2005) 193-204.
31. Baker, A.H., Edwards, D.R. and Murphy, G. Metalloproteinase inhibitors: biological actions and therapeutic opportunities. **J. Cell. Sci.** 115 (2002) 3719-3727.
32. Cheung C., Luo H., Yanagawa B., Leong H.S., Samarasekera D., Lai J.C., Suarez, A., Zhang, J. and McManus, B.M. Matrix metalloproteinases and tissue inhibitors of metalloproteinases in coxsackievirus-induced myocarditis. **Cardiovasc. Pathol.** 15 (2006) 63-74.
33. Li, J., Schwimmbeck, P.L., Tschope, C., Leschka, S., Husmann, L., Rutschow, S., Reichenbach, F., Noutsias, M., Kobalz, U., Poller, W., Spillmann, F., Zeichhardt, H., Schultheiss, H.P. and Pauschinger, M. Collagen degradation in a murine myocarditis model: relevance of matrix metalloproteinase in association with inflammatory induction. **Cardiovasc. Res.** 56 (2002) 235-247.